Magnetically Induced Depolarization of Microwave Scattering from a Laser-Generated Plasma

C.A. Galea, M.N. Shneider, A. Dogariu, and R.B. Miles

Phys. Rev. Applied **12**, 034055 — Published 27 September 2019

DOI: 10.1103/PhysRevApplied.12.034055

Magnetically Induced Depolarization of Microwave Scattering from a Laser-Generated Plasma

C. A. Galea,* M. N. Shneider, A. Dogariu, and R. B. Miles†
Department of Mechanical and Aerospace Engineering,
Princeton University, Princeton, New Jersey 08544, USA
(Dated: September 9, 2019)

The effects of a local external magnetic field on the microwave scattering from a laser-generated plasma are investigated by modeling and experiment, leading to the prediction and observation of magnetically induced depolarization of the scattered microwaves. The sample volume is localized by the small laser-generated plasma and the depolarization is shown to depend on both the magnitude and direction of the magnetic field, indicating the potential for standoff detection and measurement of vector magnetic fields in gases.

I. INTRODUCTION

In this paper, we study the effects of an external magnetic field on the microwave scattering from a laser-generated plasma and demonstrate magnetically induced depolarization of the scattered microwaves. Since the magnetically induced depolarization occurs locally at the small plasma and is shown to depend on both the magnitude and direction of the magnetic field, the discovery of this magneto-optical effect suggests a new potential technology for the standoff detection and measurement of local vector magnetic fields in gases.

Historically, a variety of magneto-optical rotation effects have been studied, including Faraday rotation [1], the Kerr magneto-optic effect [2], and the Voigt effect [3]. Unlike Faraday rotation where polarization rotation is due to propagation through an optically active medium such as plasma [4], the interaction with a small plasma, where $\lambda \gg L_p$ ($\lambda = 2\pi c/\omega$ is the wavelength of the electromagnetic radiation and L_p is the plasma length scale), can result in a magnetically induced polarization change not yet considered that is independent of propagation length. Previous theoretical investigations of the electromagnetic scattering by a small plasma in a magnetic field [5–7] examined the wave solutions of the scattered fields, but depolarization effects were not considered. Here we present a derivation of the magnetically induced depolarization effect and demonstrate this effect in experiment, hence introducing the capability of standoff measurements of local magnetic fields.

Shneider and Miles [8] investigated the microwave scattering by small plasma objects, showing that for a plasma with skin depth $\delta > L_p$, the plasma scatters the radiation as an oscillating dipole. Their findings led to a new regime of microwave scattering diagnostics including radar resonance-enhanced multi-photon ionization (Radar REMPI) [9] and Rayleigh microwave scattering (RMS) [10]. Radar REMPI has been applied to trace species detection [11], electron loss rate measurements [12], and temperature measurements in gas mixtures and flames [13–15], while RMS has been applied to time-resolved measurements of electron number density for plasma medicine applications and multi-photon ionization cross-section measurements [10, 16]. Both Radar REMPI and RMS achieve nanosecond time resolution through GHz bandwidth homodyne/heterodyne detection. In this paper, we extend these methods to the time accurate measurement of local magnetic field properties.

The magnetically induced depolarization of microwave scattering from a laser-generated plasma enables a magnetic field measurement that is localized at the small plasma and can be detected at arbitrary angles. This is in contrast to the measurement of a magnetic field via Faraday rotation, which is path integrated and requires measurement of a forward propagating beam. The measurement of a vector magnetic field via the magnetically induced depolarization effect is distinct from (but can be complementary to) remote vector magnetometers in the literature [17–20]. The proposed measurement technology brings standoff capability to magnetometry, allowing one to measure and monitor magnetic fields in environments with limited diagnostic access.

II. THEORY

To model the interaction, we consider a small plasma sphere with length scale L_p and assume the plasma to have a skin depth $\delta > L_p$. We model the effects of a polarized incident microwave field with angular frequency ω on the motion of the electrons within the main plasma body in the presence of an external magnetic field, illustrated in Fig. 1. Assuming a Maxwellian distribution of electrons, a fixed background of ions, and a spatially constant density plasma of number density n and volume V, we obtain the equation of motion for a displaced electron:

$$\ddot{\boldsymbol{\Delta r}} = -\frac{e}{m}(\boldsymbol{E_0}e^{-i\omega t} + \dot{\boldsymbol{\Delta r}} \times \boldsymbol{B_{ext}}) - \nu_m \dot{\boldsymbol{\Delta r}} - \zeta\omega_p^2 \boldsymbol{\Delta r}, \quad (1)$$

where $\boldsymbol{\Delta r}$ is the vector displacement of the electron, e/m is the electron charge-to-mass ratio, $\boldsymbol{E_0}$ is the microwave

* cgalea@princeton.edu
† Also: Department of Aerospace Engineering, Texas A&M University, College Station, Texas 77843, USA

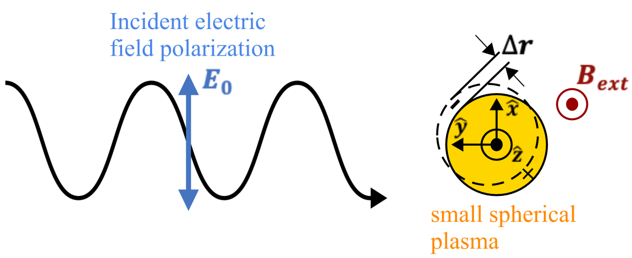

FIG. 1. Model setup for microwave scattering by a small plasma in a magnetic field. A polarized incident microwave beam interacts with a small spherical plasma, resulting in an oscillating induced dipole moment. $\boldsymbol{\Delta r}$ is the vector electron displacement from the main plasma body.

electric field amplitude, $\boldsymbol{B_{ext}}$ is the applied external magnetic field, ν_m is the electron momentum transfer collision frequency, and $\omega_p = \sqrt{ne^2/m\epsilon_0}$ is the plasma frequency. The depolarization factor ζ [21] is included to capture the effect of the plasma geometry on electric polarization; since we have assumed a spherical plasma, $\zeta_x = \zeta_y = \zeta_z = \zeta = 1/3$. We neglect the Lorentz force due to the microwave magnetic field since this is much smaller than the Lorentz force due to the microwave electric field for non-relativistic electrons.

Taking $\boldsymbol{E_0} = E_0\hat{\boldsymbol{x}}$, $\boldsymbol{B_{ext}} = B_{ext}\hat{\boldsymbol{z}}$, and $\boldsymbol{\Delta r} = \Delta x\hat{\boldsymbol{x}} + \Delta y\hat{\boldsymbol{y}} + \Delta z\hat{\boldsymbol{z}}$, we obtain a coupled system of driven damped harmonic oscillators for Δx and Δy (the displacement in $\hat{\boldsymbol{z}}$ is unaffected by the fields in this setup). We then take $\Delta x = \Delta x_0 e^{-i\omega t}$ and $\Delta y = \Delta y_0 e^{-i\omega t}$ to obtain the non-homogeneous solution due to the interaction with the microwave field. The complex amplitudes Δx_0 and Δy_0 are found to be:

$$\Delta x_0 = \frac{-\xi(e/m)E_0}{1-\omega^2\omega_c^2\xi^2}, \tag{2}$$

and

$$\Delta y_0 = \frac{i\omega\omega_c\xi^2(e/m)E_0}{1-\omega^2\omega_c^2\xi^2}, \tag{3}$$

where $\omega_c = eB_{ext}/m$ is the electron gyrofrequency and $\xi = (\zeta\omega_p^2 - \omega^2 - i\nu_m\omega)^{-1}$. We will consider the small magnetic field and low collisionality limits, i.e., keeping terms to first order in (ω_c/ω) and (ν_m/ω) with $\omega_c\omega \ll |\zeta\omega_p^2 - \omega^2|$ and $\nu_m\omega \ll |\zeta\omega_p^2 - \omega^2|$, respectively. These approximations fall well within the limits of our experiments and help to more clearly illustrate the magnetic field effect. [The full expressions in Eqs. (2) and (3) would need to be used instead if the experiment parameters do not fall into these limits.]

In the Rayleigh regime, where the receiver distance from the plasma is $R \gg \lambda \gg L_p$ and the skin depth is $\delta > L_p$ [8], the averaged scattered dipole radiation power is [22]:

$$\langle\Theta\rangle = \frac{|\ddot{\boldsymbol{d}}|^2}{6\pi\epsilon_0 c^3}, \tag{4}$$

where $\boldsymbol{d} = enV\boldsymbol{\Delta r}$ is the induced dipole moment of the small plasma. Using the principle of superposition, we can obtain the scattered electric field signal E_s (the measurable quantity in microwave scattering experiments) in the $\hat{\boldsymbol{x}}$ and $\hat{\boldsymbol{y}}$ polarizations by considering the induced dipole moment for each polarization independently:

$$E_{sx} \propto \sqrt{\langle\Theta_x\rangle} \propto |\Delta x_0|, \tag{5}$$

and

$$E_{sy} \propto \sqrt{\langle\Theta_y\rangle} \propto |\Delta y_0|, \tag{6}$$

which gives the depolarization ratio:

$$\frac{E_{sy}}{E_{sx}} = \frac{1}{\sqrt{\left(1-\zeta\left(\frac{\omega_p}{\omega}\right)^2\right)^2 + \left(\frac{\nu_m}{\omega}\right)^2}}\left(\frac{\omega_c}{\omega}\right). \tag{7}$$

The phase difference $\Delta\varphi$ between the $\hat{\boldsymbol{x}}$ and $\hat{\boldsymbol{y}}$ polarization scattered fields is found from the phase difference between Δx_0 and Δy_0:

$$\tan\Delta\varphi = \frac{1-\zeta\left(\frac{\omega_p}{\omega}\right)^2}{\left(\frac{\nu_m}{\omega}\right)}. \tag{8}$$

The angular dependence of the scattered electric field polarizations follows from the corresponding radiation patterns for the oscillating dipoles in each polarization direction [8]; we consider scattering in the $\hat{\boldsymbol{z}}$ direction since the $\hat{\boldsymbol{x}}$ and $\hat{\boldsymbol{y}}$ dipoles both radiate at a maximum in this direction. We make two conclusions based off this model: 1) in the presence of a magnetic field, we obtain a magnetically induced depolarization (in the $\boldsymbol{E_0} \times \boldsymbol{B_{ext}}$ direction) of microwave scattering, and 2) this depolarization signal is linear in $\omega_c \propto B_{ext}$ to first order. The magnetically induced depolarization of the scattering signal is illustrated in Fig. 2.

The physical mechanism behind the magnetically induced depolarization can be pictured as follows: An incoming microwave beam with an initial polarization (referred to as "E polarization") is scattered by the plasma electrons in the presence of an external magnetic field. The electrons will have an oscillation component in the E polarization direction at the microwave frequency, acting as an oscillating dipole that radiates the E polarization, but will also experience an ExB$_{ext}$ drift which oscillates at the same frequency. This results in an oscillating dipole component in the ExB$_{ext}$ direction, and hence radiation of ExB$_{ext}$ polarization, which is orthogonal to the E polarization and will be referred to as "magnetically induced depolarization". Note that the derivation of the full tensor linking $\boldsymbol{E_s}(\propto \boldsymbol{\Delta r})$ and arbitrary $\boldsymbol{E_0}$ is a simple extension of the model introduced here to the

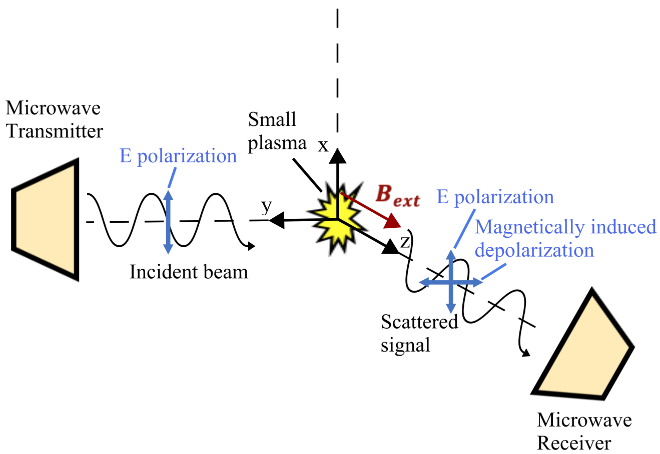

FIG. 2. Illustration of the magnetically induced depolarization effect. The incident microwave beam is polarized in what is referred to as the E polarization direction. The scattering in a magnetic field leads not only to E polarization but also to a magnetically induced depolarization component.

cases $\boldsymbol{E_0} = E_0\hat{\boldsymbol{y}}$ and $\boldsymbol{E_0} = E_0\hat{\boldsymbol{z}}$, where the former also demonstrates the magnetically induced depolarization effect while the latter is equivalent to the zero external magnetic field case, since in this case $\boldsymbol{E_0} \parallel \boldsymbol{B_{ext}}$. By applying a rotation matrix to this tensor, we can then find the expected scattering polarization ratios for an arbitrary magnetic field orientation, which could then be used to measure the vector magnetic field. If the plasma is generated by laser-induced ionization at a laser focus, the measurements can be spatially resolved, and since microwave scattering is used to probe this small laser-generated plasma, one can perform standoff measurements of the local vector magnetic field.

III. EXPERIMENT SETUP

The experiment setup follows from the illustration of Fig. 2. The small plasma ($L_p \approx 0.1$ mm) is produced via 2+1 REMPI of xenon by focusing a 0.2 mJ, 1 kHz repetition rate, 100 femtosecond laser pulse at 256 nm wavelength with a lens of 30 cm focal length into a quartz glass cell of 7 mTorr xenon with fused silica windows. The external magnetic field is generated by an electromagnet with a maximum magnetic field of $B_{max} \approx 0.08$ T. The bistatic homodyne microwave detection system is described in [10]. The transmitter emits $\omega/2\pi = 12.6$ GHz microwaves with E polarization which are scattered by the plasma ($\lambda = 2.38$ cm $\gg L_p$ ensures the plasma can be considered small). The receiver can be rotated to select either the scattered E polarization or ExB$_{ext}$ polarization, the resulting signals of which will be called the E polarization signal and the magnetically induced depolarization (also referred to as "depolarization") signal, respectively. The transmitter and receiver are both at a distance $R \approx 10$ cm away from the laser-generated plasma. We also have $\delta \approx 3$ mm along with the relevant characteristic frequencies $\omega_c/2\pi \approx 2$ GHz, $\nu_m \approx 2$ GHz, and $\omega_p/2\pi \approx 100$ GHz, ensuring that our experiment satisfies the Rayleigh regime as well as the small magnetic field and low collisionality limits described above. To ensure the plasma does not distort the external magnetic field, we require the magnetic Reynolds number $R_m = UL\mu_0\sigma$ to be less than unity, where U is the plasma fluid velocity, L is the magnetic field gradient length scale, and σ is the plasma conductivity [23]. For the small plasma in our experiment (which expands via ambipolar diffusion), we have as upper bound estimates: $U \approx 20$ km/s, $L \approx 1$ mm, and $\sigma \approx 3000\ \Omega^{-1}\text{m}^{-1}$, which result in $R_m \approx 0.06 \ll 1$. For the preceding calculations, the electron temperature $T_e \approx 2$ eV was estimated by calculating the excess energy above the ionization threshold that the 3-photon ionization (from 2+1 REMPI) process contributes, and dividing this excess energy among the three degrees of freedom of the newly freed electron. We also used the upper bound on the plasma density $n \approx 3 \times 10^{20}$ m^{-3} (full ionization case) to ensure a maximum estimate for the magnetic Reynolds number.

IV. RESULTS AND DISCUSSION

The effect of switching on an external magnetic field of $B_{ext} = B_{max}$ is shown in Fig. 3 for both the depolarization and E polarization signals. It should be noted that, 1) there is a nonzero depolarization scattering signal for $B_{ext} = 0$ due to other depolarization effects (such as scattering by the glass cell and by randomly oriented nuclear spins), and 2) there is a small phase shift between the depolarization and E polarization setups leading to a qualitative difference in the signals. Neither of these points are issues in our test, since we are focusing on the relative change due to the introduction of an external magnetic field in each case. The magnetically induced depolarization signal has a greater relative change compared to the E polarization signal, which is in agreement with our model: the depolarization signal is shown to be proportional to $(\omega_c/\omega) \approx 1/6$ [Eq. (6)], while the E polarization signal is shown to have no dependence on the magnetic field [Eq. (5)] since the effect is of second order, i.e., $(\omega_c/\omega)^2 \approx 1/36 \ll 1$. These findings suggest adjusting the receiver to the E polarization to perform measurements of quantities described in [9–16], and adjusting the receiver to the magnetically induced depolarization to detect and measure magnetic fields.

The dependence of the depolarization scattering signal on external magnetic field strength is shown in Fig. 4. The magnetic field was varied by adjusting the current applied to the electromagnet. The trend is approximately linear, which is in agreement with our first order model [Eq. (7)], and verifies that the depolarization scattering

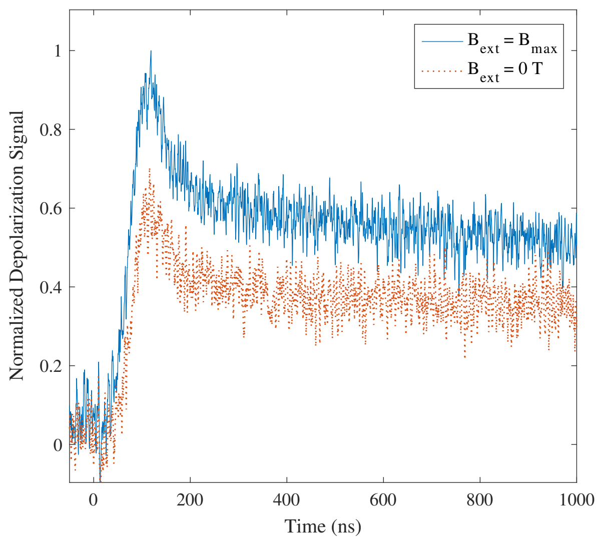

(a)

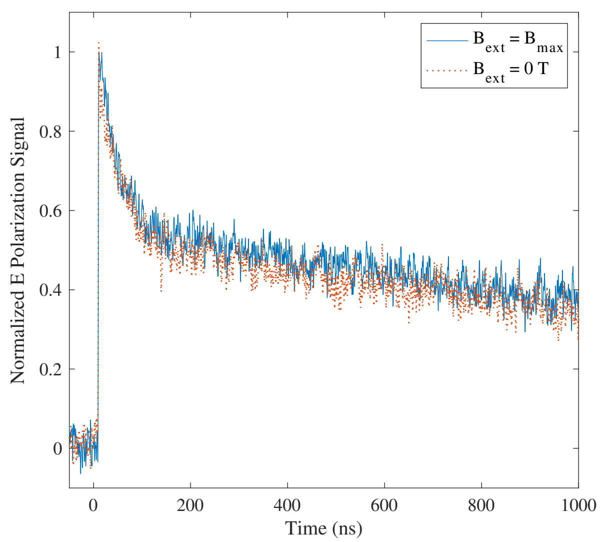

(b)

FIG. 3. Microwave scattering signal at maximum and zero external magnetic field for (a) magnetically induced depolarization and (b) E polarization. The magnetically induced depolarization signal has a greater relative change compared to the E polarization signal, which agrees with our model. The results have been averaged over 1000 laser shots.

is sensitive to the magnitude of the external magnetic field. A suitable calibration of this curve would allow quantitative measurements of the external magnetic field magnitude (since in this case $\boldsymbol{E_0} \perp \boldsymbol{B_{ext}}$), or more generally for non-orthogonal fields, quantitative measurements of the external magnetic field component orthogonal to both $\boldsymbol{E_0}$ and the receiver polarization.

Since the depolarized signal varies linearly with magnetic field strength, reversing the magnetic field direction

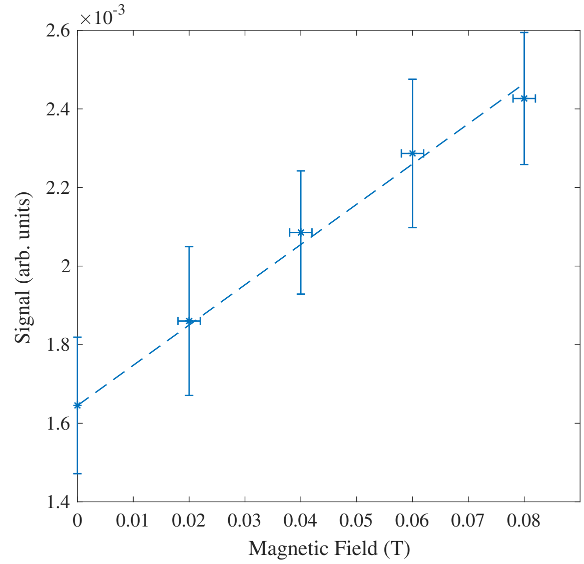

FIG. 4. Depolarization signal dependence on magnetic field strength. The trend is approximately linear, in agreement with our model. The zero magnetic field offset is due to other depolarization effects mentioned in the text. The vertical error bars represent the standard error in averaging each signal over the interval of 300-500 ns while the horizontal error bars represent the uncertainty in the current dial controlling the magnetic field strength.

(in our case, by switching the current leads) should lead to a reversal of the magnetically induced dipole, which corresponds to a 180° phase shift in the depolarization signal. Figure 5 demonstrates this effect by varying the distance of the receiver from the small plasma and plotting the signals for both positive $(+\hat{\boldsymbol{z}})$ and negative $(-\hat{\boldsymbol{z}})$ polarity magnetic field with the $B_{ext} = 0$ background signal subtracted out. The horizontal axis is the phase difference between the scattered (RF) and local oscillator (LO) microwaves, which is calculated from normalizing the receiver displacement by λ and multiplying by 360°. We see a sinusoidal dependence for each signal, with a period of 360°, corresponding to a full wavelength displacement between the RF and LO signals. The depolarization signals for positive and negative polarity external magnetic field are shown to have a relative phase difference of 180°, which is a verification of the sign reversal predicted for the magnetically induced dipole and demonstrates the capability to detect magnetic field polarity.

V. CONCLUSION

In summary, we have investigated the effect of an external magnetic field on the microwave scattering from a laser-generated plasma, where we have predicted and detected a magnetically induced depolarization of the scattered microwaves. The scattering is localized at the small laser-generated plasma and depends on the magnitude

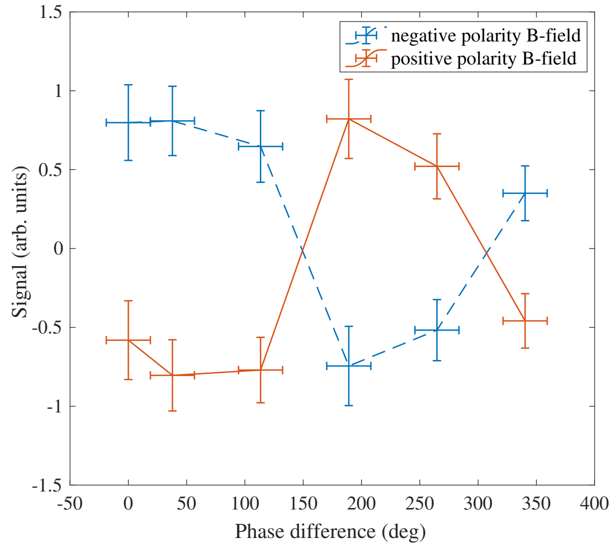

FIG. 5. Depolarization signal dependence on positive and negative polarity magnetic field for varying phase difference between the RF and LO signals, corresponding to changing the receiver distance from the small plasma. We see a sinusoidal dependence for each signal, with a relative phase difference of 180° between the signals, corresponding to a sign reversal of the magnetically induced dipole. The vertical error bars are described in Fig. 4 while the horizontal error bars represent the uncertainty in the distance measurements due to ruler resolution.

and direction of the magnetic field, showing the potential for standoff detection and measurement of local vector magnetic fields. The standoff capability of the proposed measurement technology opens the possibility of vector magnetic field measurements in limited diagnostic access environments. The nanosecond time resolution provides a time-resolved measurement of the magnetic field, which may be useful in monitoring rapidly varying magnetic field fluctuations. Since the depolarization and E polarization signals differ in their response to an external magnetic field, one can use this knowledge to either minimize magnetic field influence on a measurement quantity of interest, or maximize magnetic field influence to measure the local structure of the magnetic field. Although the small plasma was generated via REMPI in our case, in principle any small plasma could be used. The magnetically induced depolarization effect can be extended to different regimes in the electromagnetic spectrum such as terahertz or millimeter waves. It should be noted that the plasma should satisfy the Rayleigh regime if quantitative measurements are to be made, though a plasma in the Mie regime would also demonstrate the qualitative effect of magnetically induced depolarization and hence would still allow detection of the magnetic field.

ACKNOWLEDGMENTS

The authors would like to thank Nick Tkach for his help in the design and construction of the electromagnet. This research was conducted with government support from the Air Force Office of Scientific Research (AFOSR) through an SBIR with MetroLaser, Inc. and the Office of Naval Research (ONR), and with fellowship support from the Program in Plasma Science and Technology (PPST) at Princeton University.

[1] M. Faraday, I. experimental researches in electricity.–nineteenth series, Phil. Trans. R. Soc. Lond. **136**, 1 (1846).
[2] J. Kerr, Xliii. on rotation of the plane of polarization by reflection from the pole of a magnet, Phil. Mag. **3**, 321 (1877).
[3] W. Voigt, Uber das elektrische analogon des zeeman-effektes, Ann. Der Phys. **4**, 197 (1901).
[4] A. A. Dougal, J. P. Craig, and R. F. Gribble, Time-space resolved experimental diagnostics of theta-pinch plasma by faraday rotation of infrared he-ne maser radiation, Phys. Rev. Lett. **13**, 156 (1964).
[5] Y. Geng, X. Wu, and L.-W. Li, Analysis of electromagnetic scattering by a plasma anisotropic sphere, Radio Sci. **38**, 1104 (2003).
[6] Y. Ahmadizadeh, B. Jazi, and A. Abdoli-Arani, Analysis of long wavelength electromagnetic scattering by a magnetized cold plasma prolate spheroid, Waves in Random and Complex Media **23**, 336 (2013).
[7] A. K. Ram and K. Hizanidis, Scattering of electromagnetic waves by a plasma sphere embedded in a magnetized plasma, Radiation Effects & Defects in Solids **168**, 759 (2013).
[8] M. N. Shneider and R. B. Miles, Microwave diagnostics of small plasma objects, J. Appl. Phys. **98**, 033301 (2005).
[9] Z. Zhang, M. N. Shneider, and R. B. Miles, Coherent microwave rayleigh scattering from resonance-enhanced multiphoton ionization in argon, Phys. Rev. Lett. **98**, 265005 (2007).
[10] A. Shashurin, M. N. Shneider, A. Dogariu, R. B. Miles, and M. Keidar, Temporary-resolved measurement of electron density in small atmospheric plasmas, Appl. Phys. Lett. **96**, 171502 (2010).
[11] A. Dogariu and R. B. Miles, Detecting localized trace species in air using radar resonance-enhanced multiphoton ionization, Appl. Opt. **50**, A68 (2011).
[12] A. Dogariu, M. N. Shneider, and R. B. Miles, Versatile radar measurement of the electron loss rate in air, Appl. Phys. Lett. **103**, 224102 (2013).
[13] Y. Wu, J. Sawyer, Z. Zhang, and S. F. Adams, Flame temperature measurements by radar resonance-enhanced multiphoton ionization of molecular oxygen, Appl. Opt. **51**, 6864 (2012).
[14] R. B. Miles, J. B. Michael, C. M. Limbach, S. D. McGuire, T. Chng, M. R. Edwards, N. J. DeLuca, M. N. Shneider, and A. Dogariu, New diagnostic methods for

laser plasma- and microwave-enhanced combustion, Phil. Trans. R. Soc. A **373**, 0338 (2015).

[15] Y. Wu, M. Gragston, Z. Zhang, and J. D. Miller, Spatially localized, see-through-wall temperature measurements in a flow reactor using radar rempi, Opt. Lett. **42**, 53 (2017).

[16] A. Sharma, M. N. Slipchenko, M. N. Shneider, X. Wang, K. A. Rahman, and A. Shashurin, Counting the electrons in a multiphoton ionization by elastic scattering of microwaves, Sci. Rep. **8**, 2874 (2018).

[17] S. J. Seltzer and M. V. Romalis, Unshielded three-axis vector operation of a spin-exchange-relaxation-free atomic magnetometer, Appl. Phys. Lett. **85**, 4804 (2004).

[18] V. I. Yudin, A. V. Taichenachev, Y. O. Dudin, V. L. Velichansky, A. S. Zibrov, and S. A. Zibrov, Vector magnetometry based on electromagnetically induced transparency in linearly polarized light, Phys. Rev. A **82**, 033807 (2010).

[19] B. Patton, E. Zhivun, D. C. Hovde, and D. Budker, All-optical vector atomic magnetometer, Phys. Rev. Lett. **113**, 013001 (2014).

[20] T. Thiele, Y. Lin, M. O. Brown, and C. A. Regal, Self-calibrating vector atomic magnetometry through microwave polarization reconstruction, Phys. Rev. Lett. **121**, 153202 (2018).

[21] L. D. Landau and E. M. Lifshitz, *Electrodynamics of Continuous Media* (Pergamon, Amsterdam, 1984).

[22] J. D. Jackson, *Classical Electrodynamics* (Wiley, New Jersey, 1998).

[23] S. Kacenjar, M. Hausman, M. Keskinen, A. W. Ali, J. Grun, C. K. Manka, E. A. McLean, and B. H. Ripin, Magnetic field compression and evolution in laserproduced plasma expansions, Phys. Fluids **29**, 2007 (1986).